Supplementary information

The migration of Cu species over Cu-SAPO-34 and its effect on NH_3 oxidation at high temperature

Jun Wang [a] , Yu Huang [a], Tie Yu [a], Shaochun Zhu [a], Meiqing Shen [a, b]*, Wei Li[c], Jianqiang Wang [a]*

[a] Key Laboratory for Green Chemical Technology of State Education Ministry, School of Chemical Engineering & Technology, Tianjin University, Tianjin 300072, PR China

[b] State Key Laboratory of Engines, Tianjin University, Tianjin 300072, PR China

[c] General Motors Global Research and Development, Chemical Sciences and Materials Systems Lab, 3500 Mound Road, Warren, Ml 48090, USA

* Corresponding author: Jianqiang Wang

Postal address:

School of Chemical Engineering and Technology, Tianjin University, 92 Weijin Road, Nankai District, Tianjin 300072, China

Email: jianqiangwang@tju.edu.cn

Tel. / Fax. : (+86) 22-27892301

1 NH_3-TPD

Temperature programmed desorption (NH_3-TPD) experiments were performed in the same reactor for the NH_3 oxidation activity test and the same sample weight was packed. Prior to the experiments, the catalysts were pre-oxidized at 500 °C for 30 min in 5% O_2/N_2, and then 500 ppm NH_3/N_2 was purged until the outlet NH_3 con-centration was stable at 80 °C. After that, the catalysts were purged with N_2 to remove any weakly absorbed NH_3 at 80 °C. When NH_3 concentration was lower than 5 ppm, the catalysts were heated from 80 °C to 550 °C at a ramping rate of 10 °C/min. The outlet NH_3 concentrations were analysed by a Fourier Transform Infrared (FTIR) spectrometer (MKS-2030) which equipped with a 5.11 m gas cell.

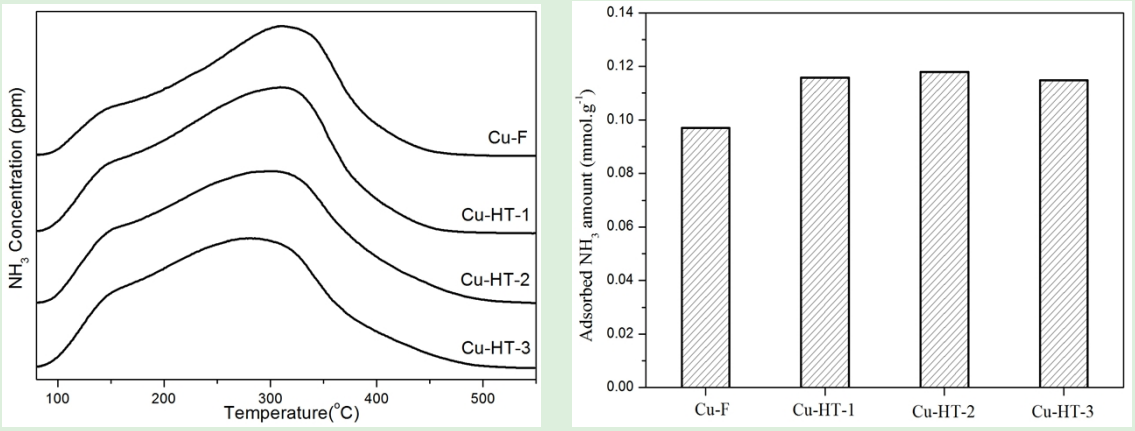

Fig. S1 The NH_3-TPD profiles and the adsorbed NH_3 content for the Cu/SAPO-34 catalysts

2 Mass Diffusion Effect

The Cu-HT-1 catalyst was used as an example to rule out the diffusion limitations. Five volume hourly space velocities (VHSV) were used to rule out the external mass transfer limitation. Fig. S2 presented the variation in NH_3 oxidation rate as a function of VHSV (1,920,000 - 4,800,000 h^{-1}) at 400 °C. The rate of NH_3 conversion initially increased with the VHSV and then leveled off at VHSV > 2,880,000 h^{-1}, indicating that the NH_3 conversion rate was not affected by the external mass transfer limitation when VHSV was higher than 2,880,000 h^{-1}. We chose the 3,600,000 h^{-1} as

the experiment condition to ensure that the reaction is free from external mass transfer limitation.

The internal diffusion limitation was examined by measuring the rates using the samples with five different particle sizes at 400 ^{o}C, as shown in Fig. S3. For the sample with the particle diameters within the range of 120 - 300 μm, the measured rates were almost constant, indicating the NH_3 conversion rates of these samples could not be affected by the intraparticle mass diffusion. The sample with 150 - 180 μm diameters (80 - 100 mesh) was chosen. However, the intracrystalline diffusion also influenced the most reactions over zeolites. Both the intraparticle and intracrystal diffusions could yield internal mass transfer effect, but the intracrystal diffusions could not be totally ruled out by measuring the rates of one catalyst with different particle sizes.

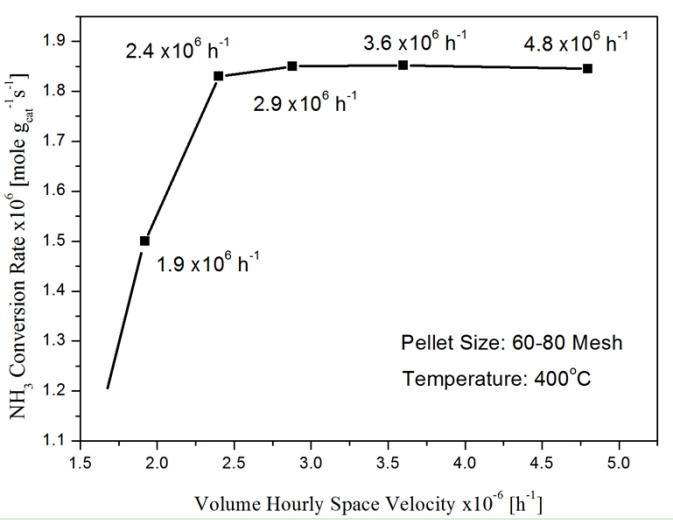

Fig. S2 NH_3 conversion rate of Cu-HT-1 catalyst for NH_3 oxidation reaction as a function of VHSV/ h^{-1} at 400 ^{o}C.

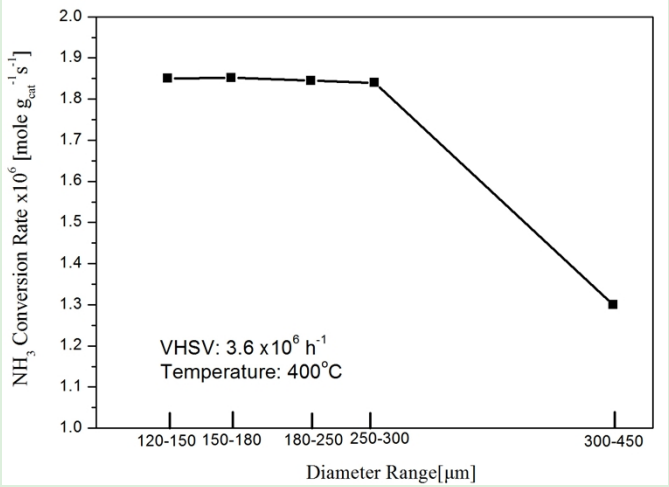

Fig. S3 NH_3 conversion rate of Cu-HT-1 catalyst for NH_3 oxidation reaction as a function of particle size at 400 °C.

3 DRIFTS of NH_3 adsorption and NH_3 oxidation

DRIFTS was performed on Nicolet 6700 FTIR equipped with a MCT detector at a resolution of 1 cm^{-1}. The total flow rate was 100 $mL \cdot min^{-1}$. Before the experiments, the samples were pretreated with 10% O_2 in He at 500 °C for 30 min and the background spectra were collected under He at the test temperature. For the adsorption experiments, the pre-treated samples were exposed to 500 ppm NH_3 for 1 h at 410 °C followed by the N_2 purge. After the spectra was stable, 5% O_2 was introduced, and the spectra was collected every 2 min during the experiment.

As shown in Fig. S4, the strong band at 1489 cm^{-1} was related to asymmetric vibration of NH_4^+ groups. The bands at 3356 cm^{-1}, 3275 cm^{-1} were assigned as N-H stretching of NH_4^+ ions H-bonded to lattice oxygens [1, 2] . It was seen that the NH_3 consumption rate for Cu-HT samples was faster than Cu-F sample from the DRIFTS result. It was worth to note that the CuO was the active site for the NH_3 oxidation, and the Cu^{2+} was the active sites for SCR reaction. And the NH_3 oxidation on Cu/SAPO-34 contained two steps: the NO generation on CuO sites and NO further consumption on Cu^{2+} sites. From our previous studies, the CuO presented no acidity and could not adsorb NH_3 from DRIFTS results. The peaks at 3279 and 1489 cm^{-1} were ascribed to the adsorbed NH_3 species on the

Brønsted acid sites. And the adsorbed NH_3 species benefited the SCR reaction than NH_3 oxidation. The gas phase NH_3 could generate NO on CuO sites, then the generated NO was further consumed on the pre-saturated Cu^{2+} sites by NH_3. In Fig. S4a, the lower NH_3 conversion rate was induced by the less Cu^{2+} sites in Cu-F sample, while the faster rate for Cu-HT sample in Figure S4b was due to its more Cu^{2+} sites. Consequently, this result was consistent with the NH_3 conversion and NO generation in Figure 10, and further confirmed the NH_3 oxidation mechanism in Scheme 1.

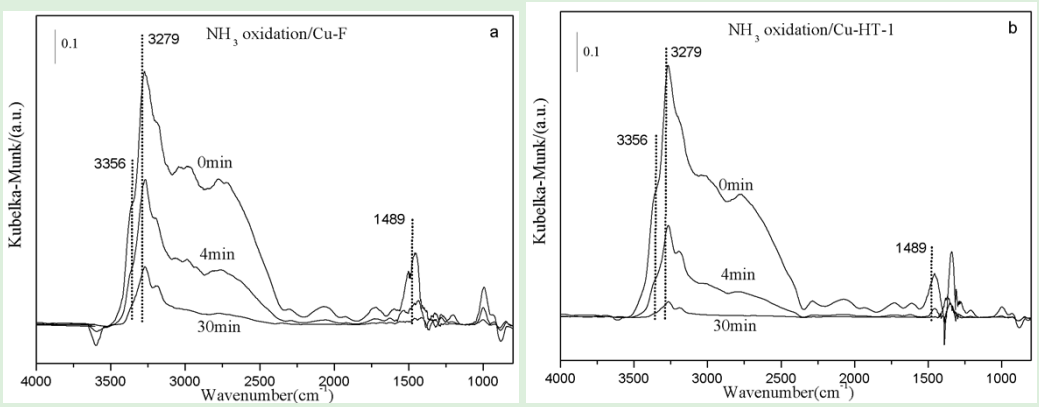

Fig. S4 The DRIFTS spectra of Cu-F (a) and Cu-HT-1 (b) for NH_3 oxidation reaction at 410 °C.

Table S1 The consuming rate of the adsorbed NH_3 in the NH_3 oxidation

Wavenumber	Sample	Consuming Rate		
		0 min	4 min	30 min
3356 cm^{-1}	Cu-F	0%	42.9%	76.3%
	Cu-HT-1	0%	76.33%	94.1%
3279 cm^{-1}	Cu-F	0%	46.8%	85.2%
	Cu-HT-1	0%	74.1%	96.4%
1489 cm^{-1}	Cu-F	0%	59.5%	88.7%
	Cu-HT-1	0%	88.7%	97.3%

4 Correlation between the pre-exponential facter and the CuO amount

The pre-exponential facter (A), which meant active site amount for NH_3 oxidation, was calculated based on the kinetic data in Fig. 12. The result in Table S2 showed that Cu-HT samples owned the similar "A/CuO amount" value, which indicated that CuO might be the NH_3 oxidation active sites of the hydrothermally treated samples. However, an intresting phenomenon was that the "A/CuO amount" value of Cu-F sample was much higher than others. It might be because that the NH_3, N_2

and O_2 molecules had kinetic diameters very close to the openings of the chabazite structures, and it was more difficult for them to react with the CuO species of the Cu-HT samples than the Cu-F sample whose most CuO was on the surface.

Table S2 The pre-exponential facter (A) and its correlation with CuO amount

Catalysts	ln A	A	A / CuO amount (mol^{-1})
Cu-F	4.892	133.22	0.6547
Cu-HT-1	3.707	40.90	0.3064
Cu-HT-2	3.446	31.36	0.3007
Cu-HT-3	3.091	22.01	0.3130

Crystal structure model of Cu/SAPO-34

The crystal structure model of Cu/SAPO-34 was shown in Scheme S1. SAPO-34 was a zeolite with the Chabazite (CHA) framework structure. And CHA structure can be described as an ABC sequence of double 6-rings of tetrahedra linked together through single 4-rings. The resulting framework is characterized by a three dimensional channel system confined by 8-membered rings. The channel intersections give rise to the so-called chabazite cage [3].

In our article, the CuO species initially existed on the external surface of the SAPO-34, and they converted into the isolated Cu^{2+} in the center of the hexagonal prism and nanosized CuO in the cavity after the hydrothermal treatment, as shown in Scheme S1.

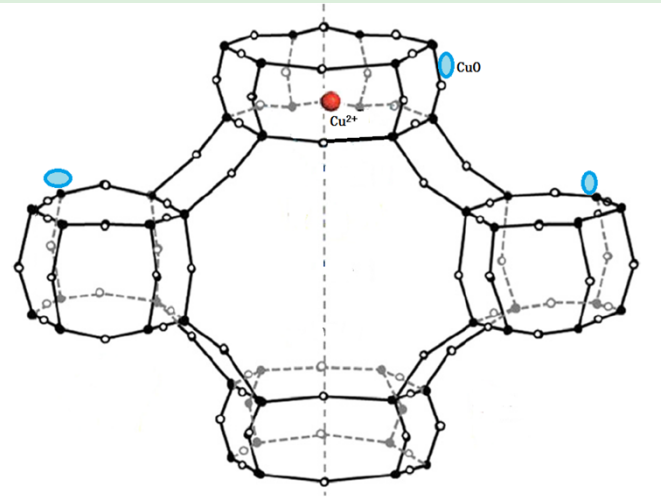

Scheme S1. Skeleton structure diagram of the unit cell of the Cu-HT samples.

Each solid circle represents an Al, P, or Si and the open circles represent oxygen.

6 XPS results of the Cu/SAPO-34 catalysts

The X-ray photoelectron spectroscopy (XPS) analysis for Cu-F and Cu-HT-3 was conducted to further understand the Cu species on the samples surface. It was carried out on a PHI-1600 ESCA system with Mg Kα source operating at 250 W. The binding energy was calibrated internally by the carbon deposit C 1s binding energy (BE) at 284.6 eV.

It was known that CuO and Cu^{2+} species of the fresh impregnated sample intended to exist on the support surface, while the Cu species of the hydrothermally treated samples mainly enriched in the bulk phase. The detection depth of the XPS analysis was about 5 nm, so the XPS signal intensity of Cu-F was higher than Cu-HT-1 as shown in Fig. S5 and it was not suitable to compare between different samples. As shown in Fig.S5, the binding energy of 934.2 eV for the Cu $2p_{3/2}$ peak was the characteristic of Cu^{2+} species, while lower binding energy of 932.1 eV was the characteristic of Cu^{+} [4-7]. No obvious Cu^{+} XPS signal was detected for the Cu-F sample, but there was a shoulder peak at BE=932.1 eV for the Cu-HT-3 sample. And the ratio of Cu^{+}/Cu^{2+} for the Cu-HT-3 was nearly 0.06 according to the integration area of Cu^{+} and Cu^{2+} peaks. Combining CO-DRIFTS, H_2-TPR and XPS results, it could be concluded that the Cu^{+}/Cu^{2+} ratios of the Cu/SAPO-34 catalysts were from 0 to 0.06 (as Table S3), which indicated that the Cu^{+} amount of the samples in our study was very little.

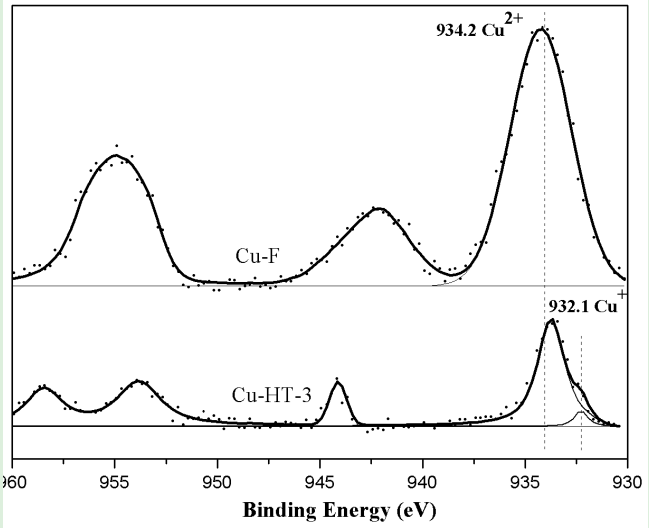

Fig. S5 The XPS spectra for the Cu-SAPO-34 catalysts.

Table S3 The Cu^{+}/Cu^{2+} ratios of the Cu/SAPO-34.

Sample	Cu^{+}/Cu^{2+} Molar Ratio [a]
Cu-F	0.007
Cu-HT-1	0.022
Cu-HT-2	0.029
Cu-HT-3	0.059

[a] analyzed by CO-DRIFTS and XPS

References:

1. G. V. A. Martins, G. Berlier, C. Bisio, S. Coluccia, H. O. Pastore and L. Marchese, *The Journal of Physical Chemistry C*, 2008, **112**, 7193.

2. A. Zecchina, L. Marchese, S. Bordiga, C. Pazè and E. Gianotti, *The Journal of Physical Chemistry B*, 1997, **101**, 10128.

3. L. Leardini, S. Quartieri and G. Vezzalini, *Microporous and Mesoporous Materials*, 2010, **127**, 219.

4. C. Ge, L. Liu, X. Yao, C. Tang, F. Gao and L. Dong, *Catalysis Science & Technology*, 2013, **3**, 1547.

5. L. Wang, J. R. Gaudet, W. Li and D. Weng, *Journal of Catalysis*, 2013, **306**, 68.

6. R. Zhang, D. Shi, Y. Zhao, B. Chen, J. Xue, X. Liang and Z. Lei, *Catalysis Today*, 2011, **175**, 26.

7. L. Liu, Z. Yao, B. Liu and L. Dong, *Journal of Catalysis*, 2010, **275**, 45.